Journal of
Composites Science

MDPI

Article

Computational Investigation of Crack-Induced Hot-Spot Generation in Energetic Composites

Xingzi Yang [1,†], Liqiang Lin [1,†], Justin Wilkerson [2] and Xiaowei Zeng [1,*]

[1] Department of Mechanical Engineering, University of Texas at San Antonio, San Antonio, TX 78249, USA; xingzi.yang@utsa.edu (X.Y.); locklin2008@gmail.com (L.L.)
[2] Department of Mechanical Engineering, Texas A&M University, College Station, TX 77843, USA; wilkerson@tamu.edu
* Correspondence: xiaowei.zeng@utsa.edu; Tel.: +1-210-458-7698
† These authors contributed equally to this work.

Abstract: The sensitivity of polymer-bonded explosives (PBXs) can be tuned through adjusting binder material and its volume fraction, crystal composition and morphology. To obtain a better understanding of the correlation between grain-level failure and hot-spot generation in this kind of energetic composites as they undergo mechanical and thermal processes subsequent to impact, a recently developed interfacial cohesive zone model (ICZM) was used to study the dynamic response of polymer-bonded explosives. The ICZM can capture the contributions of deformation and fracture of the binder phase as well as interfacial debonding and subsequent friction on hot-spot generation. In this study, a two-dimensional (2D) finite element (FE) computational model of energetic composite was developed. The proposed computational model has been applied to simulate hot-spot generation in polymer-bonded explosives with different grain volume fraction under dynamic loading. Our simulation showed that the increase of binder phase material volume fraction will decrease the local heat generation, resulting in a lower temperature in the specimen.

Keywords: polymer-bonded explosive composite; interfacial zone model; finite element simulation; crack propagation; hot-spot generation

Citation: Yang, X.; Lin, L.; Wilkerson J.; Zeng, X. Computational Investigation of Crack-Induced Hot-Spot Generation in Energetic Composites. *J. Compos. Sci.* **2021**, *5*, 210. https://doi.org/10.3390/jcs5080210

Academic Editor: Francesco Tornabene

Received: 9 July 2021
Accepted: 5 August 2021
Published: 10 August 2021

1. Introduction

Polymer-bonded explosives, also called PBXs, are composite systems in which small explosive crystals are bonded by a polymer. PBXs are developed in military affairs, aeronautics and the space industry. PBXs have many potential advantages. Polymer matrix is an elastomer and tends to absorb shocks, making the PBX very insensitive to accidental detonation. Hard polymers can produce PBX that is very rigid and maintains a precise engineering shape even under severe stress. The binder also allows PBXs to be pressed and machined to desired shapes and sizes [1]. To understand the behavior/performance of PBXs, an extensive amount of research work has been carried out in terms of both experiment and numerical simulation. Palmer et al. [2,3] investigated and analyzed the distribution of stress, failure strength and fracture behavior of PBXs with different compositions. It is important to keep a low sensitivity and high explosiveness when optimizing the mechanical properties. In their experiment, compositions based on microsized crystals were the strongest. Other studies focused on the characterization of heterogeneous microstructures [4,5], fracture and deformation [6–9], the effects of temperature and strain-rate [10] and the correlation between microstructure and fracture behavior [11].

Microcrack evolution inside PBXs was considered to be the most important phenomenon during impact [12,13], and the friction between microcrack surfaces was considered to govern the ignition. Bennett et al. [14] proposed a viscoelastic cracking constitutive model (visco-SCRAM) and which was widely used. Liu and Chen applied the visco-SCRAM to non-shock impacts to relate the impact velocity to ignition time, sample size and

the influence of the projectile shape [15,16]. Reaugh et al. [17] developed a high explosive response to the mechanical stimulus model (HERMES) by simultaneously considering the yield strength, the equation of state, particle fractures and also built up the relationship between cracks and ignition. Barua and Zhou [1,18,19] developed a Lagrangian framework based on the cohesive finite-element model to analyze the crack evolution of the interface between the explosive crystal and polymer and to further investigate the ignition induced by the shock wave generated from the high-velocity impact. The obtained microstructure-response relationship can be used to evaluate the initiation sensitivity of energetic composites [20]. Xiao et al. [16] implemented the model in ABAQUS to predict the damage responses of PBX under impact loading. The computational results were verified by experiments. He et al. [21] used the two-dimensional (2D) graphene nanoplatelets (GNPs) to enhance the thermal conductivity of PBX. Banerjee et al. [22] applied the Lagrangian formula to study the effect of particle/binder debonding on the elastic modulus of the glass-Estane PBX simulant. Wu et al. [23] used the rate-dependent viscoelastic cohesion zone model of the adhesive and the continuous damage model of the HMX grains to simulate the response of the PBX 9501 in the Brazilian compression test. These findings indicate that grain fracture and grain/binder debonding play an important role in the failure of PBX. The behavior of the adhesive is extremely important because it will affect the mechanical response of the polymer composite. The stiffness of the adhesive is five orders of magnitude lower than the stiffness of the explosive crystal [24]. Parker et al. [25] find that there is some safety benefit for having binders in HMX, especially when the binder is thermally stable.

As we know, the material interface plays an important role in the material damage process in this kind of composite materials. We applied the recently developed generalized interfacial zone model to investigate the damage process in energetic composite materials. A computational model and simulation tool has been developed for more advanced study since different interface behaviors can be modeled. In this research, we built a 2D computational model and developed custom-designed simulation software to obtain a better understanding of the correlation between grain-level failure and hot-spot generation in energetic composites as they undergo mechanical and thermal processes subsequent to impact. The interfacial cohesive zone model (ICZM) was used to model different interfaces in the model and to simulate hot-spot generation in polymer-bonded explosives with different grain volume fraction under dynamic loading. Our simulation results showed that the volume fraction of binder phase material play an important role on the local heat generation.

2. Computation Model

2.1. Geometric Model and Boundary Conditions

In this study, we develop a 2D computational model of energetic composite. The proposed computational model contains grain, a binder phase and an interface between grain and binder. To create the geometry of this computational model, we generate randomly distributed mineral tablets via Voronoi tessellation [26]. Then, we recess the edges of each original polycrystalline grain in parallel towards the centroid of the grains with a designated distance to generate a thin layer binder phase between adjacent grains. After that, we embedded interfaces between the binder phase and grain to govern the interface behavior. To simulate crack initiation and propagation of the model material, cohesive zones are also built in grain and binder phase. The geometry structure is shown in Figure 1. The dimension of the 2D model is $L_x \times L_y = 3$ mm $\times$ 3 mm with 144 grains. As shown in Figure 1, a velocity boundary condition with a boundary velocity 2500 m/s is applied on the top and bottom edges of the specimen and the left and right edges of the specimen are set as free boundary conditions.

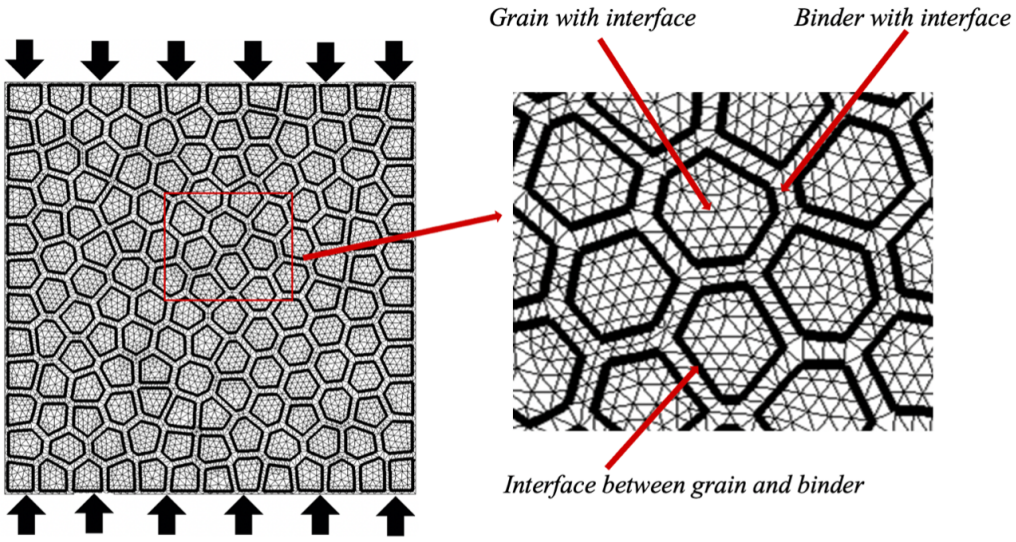

Figure 1. Geometric model with interface and boundary conditions.

2.2. Interfacial Zone Model

Polymer-bonded explosives contain grain and binder. To describe the interface deformation behavior, an interfacial zone model was proposed to mimic various interfacial behaviors. The interfacial zone is widely used to study composite material failure process [27–35]. The proposed interfacial zone model provides a numerical tool to study material response through defining different material interface behaviors [35,36]. Figure 2 shows the traction–separation relations in surface normal and tangential directions, which were used to govern the interfacial behaviors. The relationship includes four deformation stages in normal direction: compressive contact stage $(0 \sim \delta_0)$, elastic stage $(\delta_0 \sim \delta_c)$, damage stage $\left(\delta_c \sim \delta_f\right)$ and complete failure stage $\left(\delta_f \sim +\infty\right)$. In the shear traction–separation law, it has similar deformation stages: elastic stage $(0 \sim \delta_c)$, damage stage $\left(\delta_c \sim \delta_f\right)$ and complete failure stage $\left(\delta_f \sim \infty\right)$ with symmetry in both directions. The interface toughness is the area under the traction–separation curve and the normal and shear interface toughness are respectively defined as:

$$\varnothing_n = \int_{\delta_0}^{\delta_{\mathrm{fn}}} \mathbf{T}\mathrm{d}\boldsymbol{\delta} \tag{1}$$

$$\varnothing_t = \int_{0}^{\delta_{\mathrm{ft}}} \mathbf{T}\mathrm{d}\boldsymbol{\delta} \tag{2}$$

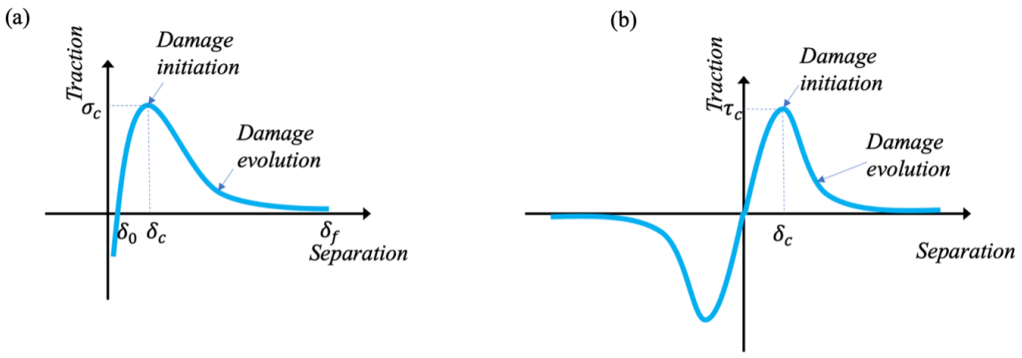

Figure 2. Traction–separation relations used to describe interfacial behaviors: (**a**) normal direction; (**b**) tangential direction.

The interfacial traction–separation laws take the following form:

$$T_n = \begin{cases} \sigma_c \left(\frac{\Delta_n - \delta_0}{\delta_{dn} - \delta_0}\right) \exp(1) \exp\left(-\frac{\Delta_n - \delta_0}{\delta_{dn} - \delta_0}\right) & \Delta_n \le \delta_{dn} \\ \sigma_c \left(\frac{\delta_{fn} - \Delta_n}{\delta_{fn} - \delta_n}\right)^{p_n} & \delta_{dn} < \Delta_n < \delta_{fn} \\ 0 & \Delta_n \ge \delta_{fn} \end{cases} \tag{3}$$

$$T_t = \begin{cases} \tau_c \sqrt{\exp(1)} \left(\frac{\Delta_t}{\delta_{dt}}\right) \exp\left(-\frac{\Delta_t^2}{2\delta_{dt}^2}\right) & 0 \le |\Delta_t| \le \delta_{dt} \\ \tau_c \frac{\Delta_t}{|\Delta_t|} \left(\frac{\delta_{ft} - |\Delta_t|}{\delta_{ft} - \delta_{dt}}\right)^{p_t} & \delta_{dt} < |\Delta_t| < \delta_{ft} \\ 0 & \Delta_n \ge \delta_{ft} \end{cases} \tag{4}$$

where σ_c and τ_c are cohesive strength in the normal and tangential direction, respectively; δ_{dn} and δ_{dt} are critical separation. The δ_{fn} and δ_{ft} are normal and tangential failure separation. The δ_0 is the equilibrium position and $\exp(1) = 2.71828$. The variables n and t represent normal and tangential direction, respectively. In this study, we applied zero-thickness cohesive interfacial zone to model the interface, which was governed by the traction–separation law.

2.3. Heat Generation in the Model

The frictional work produces a hot spot, releases heat and then temperature is increased around the crack. The rate at which heat is generated at the frictional contact is [37]:

$$h = \mathbf{t} \cdot [\mathbf{v}] \tag{5}$$

where $\mathbf{t}$ is the contact traction and $[\mathbf{v}]$ is the jump in velocity across the contact.

The generation of heat increases the heat at the nodes on the contact surfaces.

$$\frac{h_1}{h_2} = \frac{\sqrt{k_1 \rho_1 c_1}}{\sqrt{k_2 \rho_2 c_2}} \tag{6}$$

where h_i represents the heat rate, k_i, ρ_i and c_i represent the thermal conductivities, mass densities and the heat capacity of the two contacting materials $(i = 1, 2)$.

To evaluate the temperature rise at the node pair, a thermal energy averaging scheme is used [1]

$$\Delta T = \frac{\sum_{i=1}^{n} h_i}{\sum_{j=1}^{n} m_j c_j} \tag{7}$$

where n represents the number of the node pair, m_j is the lumped mass and c_j is the lumped thermal capacitance of the j th node at the junction.

2.4. Finite Element (FE) Implementations

Following standard procedures and neglecting the body force, the principle of virtual work of finite element formulation can be written as:

$$\int_{\Omega} \rho \ddot{\mathbf{u}} \cdot \delta \mathbf{u} d\Omega = \int_{\Gamma_{ext}} \overline{\mathbf{T}} \cdot \delta \mathbf{u} dS + \int_{\Gamma_{\text{inter}}} \mathbf{T}^{\text{inter}} \bullet \delta \Delta dS - \int_{\Omega} \mathbf{P} : \delta \mathbf{F} d\Omega \tag{8}$$

where $\Omega, \Gamma_{\text{inter}}, \Gamma_{\text{ext}}$ are the volume, interface boundary and external traction boundary of element in the reference configuration, respectively; $\mathbf{P}$ is the first Piola–Kirchhoff stress tensor; $\mathbf{F}$ is the deformation gradient; Δ denotes the interfacial displacement jump across the interfaces; $\overline{\mathbf{T}}$ denotes the external traction vector and $\mathbf{T}^{\text{inter}}$ is the interfacial bonding traction vector; ρ represents the material density in the reference configuration.

2.5. Material Properties

In our study, the material models of grain and binder phase are elastic. The material properties for grain and binder phase are listed in Table 1. The binder is a common

polymer known as ESATNE 5703 and used in explosive PBX 9501. The grain material is HMX(octahydro-1,3,5,7-tetranitro-1,3,5,7-tetrazocine). The parameters of different interface property are listed in Table 2.

Table 1. Material properties [1].

Material Property	HMX	Estane
Young's modulus	25,325.0 MPa	0.77 MPa (Loading modulus)
Density	1.58 g cm^{-3}	0.90 g cm^{-3}
Specific heat	1254.0 J kg^{-1} K^{-1}	1500.0 J kg^{-1} K^{-1}
Poisson's ratio	0.250	0.499

Table 2. Parameters of interface property [1].

Parameters of Interface	Grain/Grain	Binder/Binder	Grain/Binder
σ_n(MPa)	100	38.4	35
$(\delta_{dn} - \delta_0)$ (μm)	5.0	10.0	4.62
$\left(\delta_{fn} - \delta_0\right)$ (μm)	5.0	10.0	4.62
p_n	0.0	0.0	0.0
τ_t (MPa)	100	38.4	35
δ_{dt} (μm)	5.0	10.0	4.62
δ_{ft} (μm)	5.0	10.0	4.62
p_t	0.0	0.0	0.0

3. Simulation Results

In material science and solid mechanics, material deformation and failure are very important to the determination of the integrity of the structure. Knowing the material failure modes can help us to improve the material's structure and protect it against potential failure. Numerical simulations were performed to investigate the failure process in the composite material. All simulations were conducted by using a custom-designed finite element package, which was developed by Zeng and his co-workers [30,31,35,36,38,39] by using the Fortran computer language. The verification of the code and convergence study on specimen size and mesh size were conducted in our previous studies in composite materials with similar structures [27,29,32].

In cohesive finite element modeling, when the separation at the interface reaches its critical separation (δ_c), the crack will initiate. As more cracks initiate and nucleate, they will coalesce to form big cracks. Through analysis of the fracture pattern in the specimen, we found that the cracks initiated at the interface between grain and binder. As loading increases, intergranular cracks propagated along an inclined angle via relative sliding between grain and blinder (Figure 3).

As the loading keeps increasing, we observed that some hot spots were generated at the damaged interface between grain and binder as shown in Figure 4. When the intergranular cracks grows, the specimen releases energy near the crack. In the stress concentration area, more likely the interfaces will reach their critical separation. Then crack will initiate and propagate as loading keeps increasing. When damage happens at a specific location, the stress will be released and a hot spot will be generated. The temperature increase is due to interface damage as shown in Figure 4.

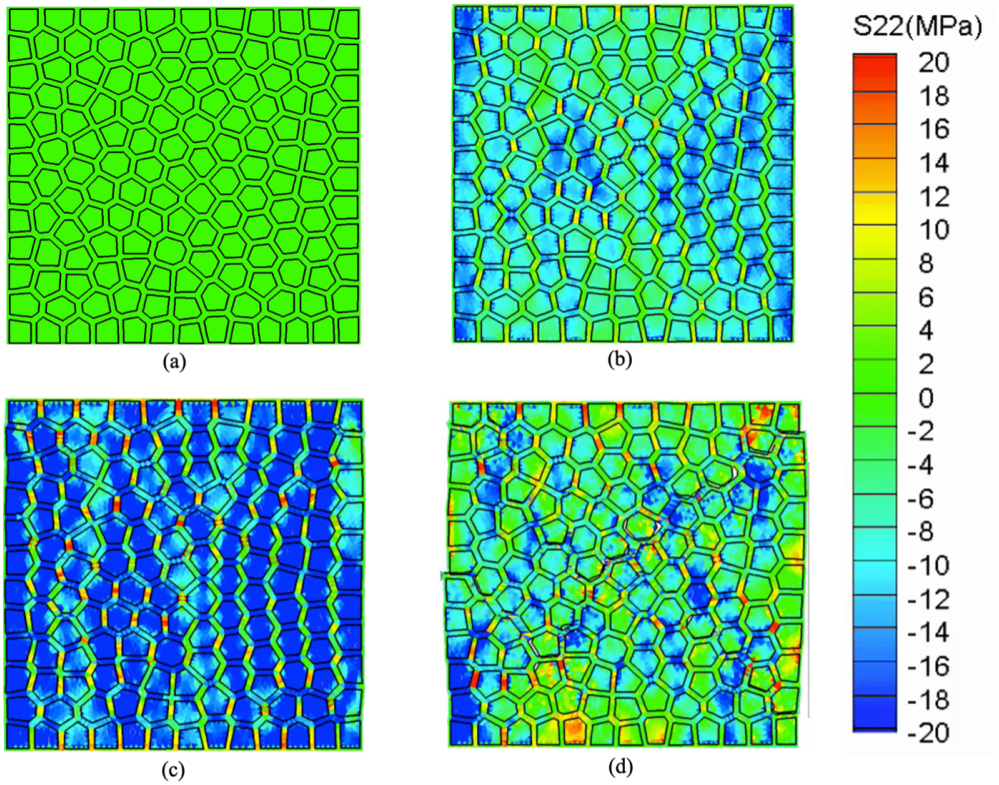

Figure 3. Snapshots of stress distribution (σ_{22}) under impact loading: (**a**) initial stage; (**b**) stress concentration; (**c**) crack initiation; (**d**) crack coalescence.

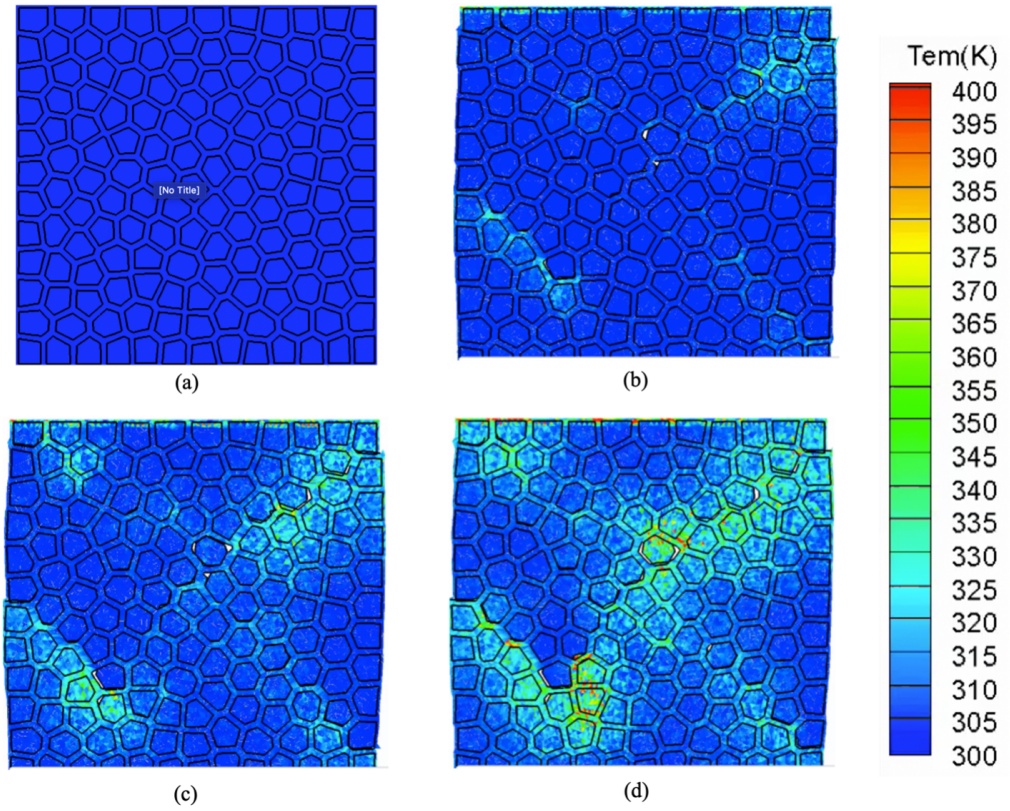

Figure 4. Snapshots of temperature distribution in specimen:(**a**) initial stage; (**b**) crack initiation; (**c**) crack propagation; (**d**) final stage. As loading increases, the hot-spot was generated at the damaged interface between grain and binder.

In this study, we used an interfacial zone model to study the dynamic response of polymer-bonded explosives. The volume fraction of grain and binder phase play an important role on the material response. We chose three different grain volume fractions of 64%, 75% and 82% to determine the stress–strain curves at different grain volume fraction. Correspondingly, the binder phase volume fractions are 36%, 25% and 18%. From the simulation results, we found that both strength and stiffness increase as grain volume fraction increases within the tested range. Further, the strain corresponding to the peak stress is dependent on binder material volume fraction. As the binder content increases, this strain also increased as shown in Figure 5, which is in good agreement with other studies [1].

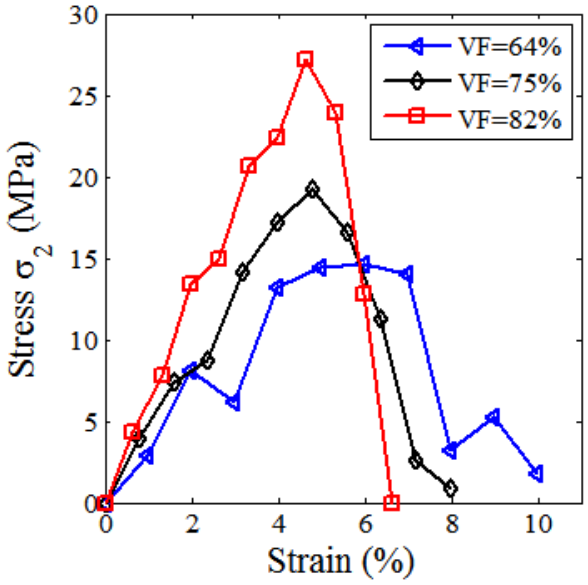

Figure 5. Stress–strain curves at different grain volume fraction. The results indicate that ultimate stress will increase as the grain volume fraction increases.

From Figure 6, we observed that the higher volume fraction of grain will generate a hot spot with higher temperature. This is because more damage will take place at the interface between grain and blinder. The possible reason is that as the grain volume fraction increases, the grain and binder interface area will increase, so more cracks may happen along the interface, more cracks will release more energy so the temperature will be higher as shown in Figure 6.

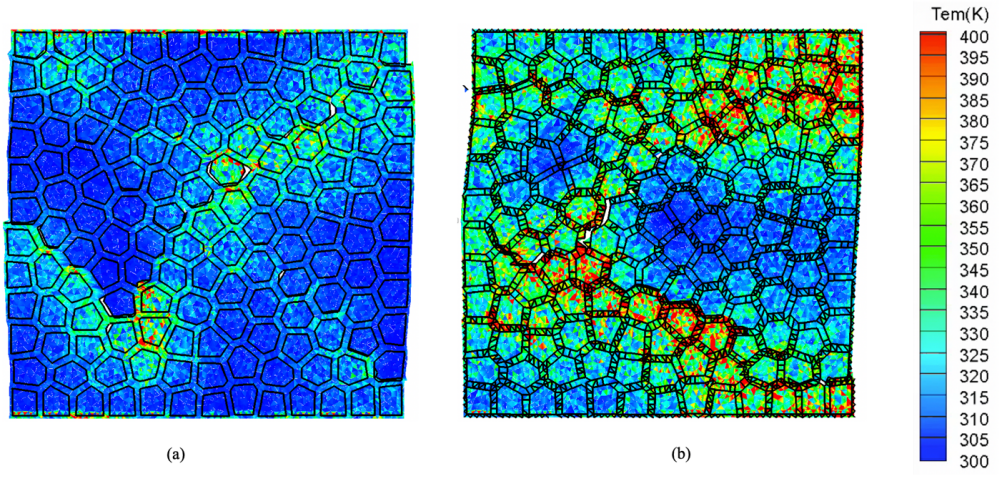

Figure 6. Hot-spot generation with different grain volume fraction under compressive loading (**a**) Vol = 64%; (**b**) Vol = 82%.

4. Discussion and Conclusions

A 2D computational model of energetic composite was developed. The proposed computational model has been applied to simulate hot-spots generation in polymer-bonded explosives with different grain volume fraction under dynamic loading. The failure modes were closely coincided with the result from experiment. Our simulation results showed that as the grain volume fraction increases in the tested range, both stiffness and ultimate stress will increase, also the temperature will increase at the hot-spot generation region. The current work is a primitive study of local heat generation in energetic composites due to cracks. In our future study, we will consider fully thermal–mechanical coupling in this material. The current study provides a numerical tool and may open a door for more advanced study of energetic composites through adjusting binder material and volume fraction, crystal composition and morphology, e.g., using carbon nanotube reinforced composite materials can provide additional dissipation pathways for impact energy as well as conduct heat away from energy localizations.

Author Contributions: Conceptualization, J.W. and X.Z.; methodology, L.L. and X.Z.; software, L.L. and X.Z.; validation, L.L. and X.Y.; formal analysis, L.L. and X.Y.; investigation, L.L. and X.Y.; resources, X.Z.; data curation, L.L. and X.Y.; writing—original draft preparation, L.L. and X.Y.; writing—review and editing, X.Z. and J.W.; visualization, L.L. and X.Y.; supervision, X.Z.; project administration, J.W. and X.Z.; funding acquisition, J.W. and X.Z. All authors have read and agreed to the published version of the manuscript.

Funding: This research was funded by Air Force Office of Scientific Research grant number FA9550-16-1-0204.

Institutional Review Board Statement: Not applicable.

Informed Consent Statement: Not applicable.

Data Availability Statement: The data presented in this study are available on request from the corresponding author. The data are not publicly available due to UTSA data sharing policy.

Acknowledgments: This work is supported by a grant from the Air Force Office of Scientific Research (grant number FA9550-16-1-0204). Valuable discussions with Babak Ravaji are gratefully acknowledged.

Conflicts of Interest: The authors declare no conflict of interest.

References

1. Barua, A.; Zhou, M. A Lagrangian framework for analyzing microstructural level response of polymer-bonded explosives. *Model. Simul. Mater. Sci. Eng.* **2011**, *19*, 055001. [CrossRef]
2. Palmer, S.; Field, J. The deformation and fracture of β-HMX. *Proc. R. Soc. Lond. Math. Phys. Sci.* **1982**, *383*, 399–407.
3. Palmer, S.J.P.; Field, J.E.; Huntley, J.M. Deformation, Strengths and Strains to Failure of Polymer Bonded Explosives. *Proc. Math. Phys. Sci.* **1993**, *440*, 399–419.
4. Liu, G.; Yu, H. Stereological characterization of particle contiguity. *J. Microsc.* **1996**, *181*, 82–87. [CrossRef]
5. Skidmore, C.; Phillips, D.; Son, S.; Asay, B. Characterization of HMX particles in PBX 9501. In *AIP Conference Proceedings*; American Institute of Physics: College Park, MD, USA, 1998; pp. 579–582.
6. Berghout, H.; Son, S.; Skidmore, C.; Idar, D.; Asay, B. Combustion of damaged PBX 9501 explosive. *Thermochim. Acta* **2002**, *384*, 261–277. [CrossRef]
7. Liu, C. Fracture of the PBX 9501 high explosive. In *AIP Conference Proceedings*; American Institute of Physics: College Park, MD, USA, 2004; pp. 786–791.
8. Rae, P.; Goldrein, H.; Palmer, S.; Field, J.; Lewis, A. Quasi–static studies of the deformation and failure of β–HMX based polymer bonded explosives. *Proc. R. Soc. Lond. Ser. Math. Phys. Eng. Sci.* **2002**, *458*, 743–762. [CrossRef]
9. Williamson, D.; Palmer, S.; Proud, W. Fracture studies of PBX simulant materials. In *AIP Conference Proceedings*; American Institute of Physics: College Park, MD, USA, 2006; pp. 829–832.
10. Cady, C.; Blumenthal, W.; Gray III, G.; Idar, D. Mechanical properties of plastic-bonded explosive binder materials as a function of strain-rate and temperature. *Polym. Eng. Sci.* **2006**, *46*, 812–819. [CrossRef]
11. Chen, P.; Huang, F.; Ding, Y. Microstructure, deformation and failure of polymer bonded explosives. *J. Mater. Sci.* **2007**, *42*, 5272–5280. [CrossRef]

12. Chidester, S.; Tarver, C.; DePiero, A.; Garza, R. Single and multiple impact ignition of new and aged high explosives in the Steven impact test. In *AIP Conference Proceedings*; American Institute of Physics: College Park, MD, USA, 2000; pp. 663–666.
13. Idar, D.J.; Straight, J.W.; Osborn, M.A.; Coulter, W.L.; Buntain, G.A. Low amplitude impact of damaged PBX 9501. In *AIP Conference Proceedings*; American Institute of Physics: College Park, MD, USA, 2000; pp. 655–658.
14. Bennett, J.G.; Haberman, K.S.; Johnson, J.N.; Asay, B.W. A constitutive model for the non-shock ignition and mechanical response of high explosives. *J. Mech. Phys. Solids* **1998**, *46*, 2303–2322. [CrossRef]
15. Liu, R.; Chen, P. Modeling ignition prediction of HMX-based polymer bonded explosives under low velocity impact. *Mech. Mater.* **2018**, *124*, 106–117. [CrossRef]
16. Xiao, Y.; Sun, Y.; Zhen, Y.; Guo, L.; Yao, L. Characterization, modeling and simulation of the impact damage for polymer bonded explosives. *Int. J. Impact Eng.* **2017**, *103*, 149–158. [CrossRef]
17. Reaugh, J.E.; White, B.W.; Curtis, J.P.; Springer, H.K. *Theory, Solution Methods, and Implementation of the HERMES Model*; Technical Report; Lawrence Livermore National Lab. (LLNL): Livermore, CA, USA, 2017.
18. Barua, A.; Horie, Y.; Zhou, M. Microstructural level response of HMX–Estane polymer-bonded explosive under effects of transient stress waves. *Proc. R. Soc. Math. Phys. Eng. Sci.* **2012**, *468*, 3725–3744. [CrossRef]
19. Barua, A.; Kim, S.; Horie, Y.; Zhou, M. Ignition criterion for heterogeneous energetic materials based on hotspot size-temperature threshold. *J. Appl. Phys.* **2013**, *113*, 064906. [CrossRef]
20. Barua, A.; Horie, Y.; Zhou, M. Energy localization in HMX-Estane polymer-bonded explosives during impact loading. *J. Appl. Phys.* **2012**, *111*, 054902. [CrossRef]
21. He, G.; Yang, Z.; Zhou, X.; Zhang, J.; Pan, L.; Liu, S. Polymer bonded explosives (PBXs) with reduced thermal stress and sensitivity by thermal conductivity enhancement with graphene nanoplatelets. *Compos. Sci. Technol.* **2016**, *131*, 22–31. [CrossRef]
22. Banerjee, B.; Cady, C.M.; Adams, D.O. Micromechanics simulations of glass–estane mock polymer bonded explosives. *Model. Simul. Mater. Sci. Eng.* **2003**, *11*, 457. [CrossRef]
23. Yan-Qing, W.; Feng-Lei, H. A micromechanical model for predicting combined damage of particles and interface debonding in PBX explosives. *Mech. Mater.* **2009**, *41*, 27–47. [CrossRef]
24. Iqbal, M.; Li-Mayer, J.; Lewis, D.; Connors, S.; Charalambides, M. Mechanical characterization of the nitrocellulose-based visco-hyperelastic binder in polymer bonded explosives. *Phys. Fluids* **2020**, *32*, 023103. [CrossRef]
25. Parker, G.R.; Heatwole, E.M.; Holmes, M.D.; Asay, B.W.; Dickson, P.M.; McAfee, J.M. Deflagration-to-detonation transition in hot HMX and HMX-based polymer-bonded explosives. *Combust. Flame* **2020**, *215*, 295–308. [CrossRef]
26. Lin, L.; Wang, X.; Zeng, X. Geometrical modeling of cell division and cell remodeling based on Voronoi tessellation method. *CMES Comput. Model. Eng. Sci.* **2014**, *98*, 203–220.
27. Maghsoudi-Ganjeh, M.; Lin, L.; Wang, X.; Zeng, X. Computational investigation of ultrastructural behavior of bone using a cohesive finite element approach. *Biomech. Model. Mechanobiol.* **2019**, *18*, 463–478. [CrossRef]
28. Maghsoudi-Ganjeh, M.; Lin, L.; Wang, X.; Zeng, X. Bioinspired design of hybrid composite materials. *Int. J. Smart Nano Mater.* **2019**, *10*, 90–105. [CrossRef]
29. Lin, L.; Wang, X.; Zeng, X. The role of cohesive zone properties on intergranular to transgranular fracture transition in polycrystalline solids. *Int. J. Damage Mech.* **2017**, *26*, 379–394. [CrossRef]
30. Lin, L.; Dhanawade, R.; Zeng, X. Numerical simulations of dynamic fracture growth based on a cohesive zone model with microcracks. *J. Nanomech. Micromech.* **2014**, *4*, B4014003. [CrossRef]
31. Lin, L.; Zeng, X. Computational modeling and simulation of spall fracture in polycrystalline solids by an atomistic-based interfacial zone model. *Eng. Fract. Mech.* **2015**, *142*, 50–63. [CrossRef]
32. Lin, L.; Samuel, J.; Zeng, X.; Wang, X. Contribution of extrafibrillar matrix to the mechanical behavior of bone using a novel cohesive finite element model. *J. Mech. Behav. Biomed. Mater.* **2017**, *65*, 224–235. [CrossRef] [PubMed]
33. Maghsoudi-Ganjeh, M.; Lin, L.; Wang, X.; Wang, X.; Zeng, X. Computational Modeling of the Mechanical Behavior of 3D Hybrid Organic–Inorganic Nanocomposites. *JOM* **2019**, *71*, 3951–3961. [CrossRef]
34. Maghsoudi-Ganjeh, M.; Lin, L.; Yang, X.; Zeng, X. Computational modeling and simulation of bioinspired nacre-like composites. *J. Mater. Res.* **2021**, *36*, 2651–2661. [CrossRef]
35. Lin, L.; Wang, X.; Zeng, X. Computational modeling of interfacial behaviors in nanocomposite materials. *Int. J. Solids Struct.* **2017**, *115*, 43–52. [CrossRef] [PubMed]
36. Lin, L.; Wang, X.; Zeng, X. An improved interfacial bonding model for material interface modeling. *Eng. Fract. Mech.* **2017**, *169*, 276–291. [CrossRef]
37. Camacho, G.T.; Ortiz, M. Computational modelling of impact damage in brittle materials. *Int. J. Solids Struct.* **1996**, *33*, 2899–2938. [CrossRef]
38. Zeng, X.; Li, S. Application of a multiscale cohesive zone method to model composite materials. *Int. J. Multiscale Comput. Eng.* **2012**, *10*, 391–405. [CrossRef]
39. Zeng, X.; Li, S. A multiscale cohesive zone model and simulations of fractures. *Comput. Methods Appl. Mech. Eng.* **2010**, *199*, 547–556. [CrossRef]